supplemental material for

# Topological dual double node-line semimetals NaAlSi(Ge) and their potential as cathode material for sodium ion batteries

X. Yi,[1] W. Q. Li,[1] P. Zhou,[1,*] Z. H. Li,[1] Z. S. Ma,[1] and L. Z. Sun[1,†]

[1]*Hunan Provincial Key laboratory of Thin Film Materials and Devices, School of Material Sciences and Engineering, Xiangtan University, Xiangtan 411105, China*

(Dated: October 7, 2019)

## I. THE IRREDUCIBLE REPRESENTATIONS (IRS) AND TABLE OF CHARACTERS.

The identified irreducible representations of the two bands around the Fermi level along the two high symmetric lines are shown clearly in fig.S1(a). The table of characters for identified irreducible representations of the Point Group is listed in fig.S1(b). For X-Γ high symmetry line, the results indicate that the irreducible representations for the two crossing bands of $C_1$ are $\Gamma_2$ and $\Gamma_4$, respectively, whereas the irreducible representations for the two crossing bands of $C_3$ are $\Gamma_1$ and $\Gamma_4$, respectively. The character values of $\Gamma_1$, $\Gamma_2$, $\Gamma_3$ and $\Gamma_4$ are 1, 1, -1, and -1 for the mirror symmetry corresponding to the $k_z = 0$ planes. But along the high symmetry line of Γ-M, the irreducible representations for the two crossing bands of $C_2$ are $\Gamma_3$ and $\Gamma_4$, respectively, whereas the irreducible representations for the two crossing bands of $C_4$ are $\Gamma_1$ and $\Gamma_3$, respectively. And its character values of $\Gamma_1$, $\Gamma_2$, $\Gamma_3$ and $\Gamma_4$ are 1, -1, -1, and 1 for the mirror symmetry corresponding to the $k_z = 0$ planes. The bands crossing points $C_1$, $C_2$, $C_3$ and $C_4$ show opposite mirror symmetric eigenvalues, thus the band crossings are stable due to the protection by the mirror symmetry.

(a)

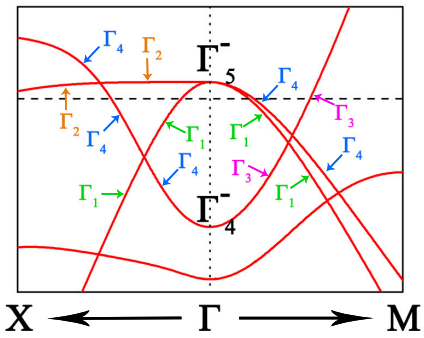


(b)

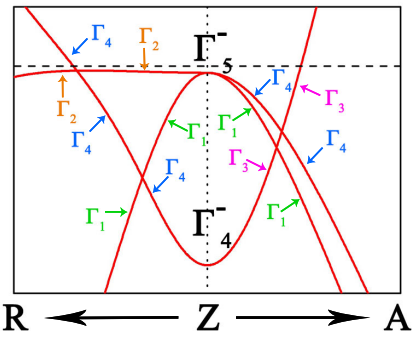


(c)

The table of characters

| repr. | $E$ | $C_2$ | $\sigma_v$ | $\sigma'_v$ |
|---|---|---|---|---|
| $\Gamma_1$ | 1 | 1 | 1 | 1 |
| $\Gamma_2$ | 1 | -1 | 1 | -1 |
| $\Gamma_3$ | 1 | 1 | -1 | -1 |
| $\Gamma_4$ | 1 | -1 | -1 | 1 |

Figure S1: (color online) (a) The irreducible representations (IRs) of the energy bands around Γ point). (b)Character table for group $C_{2v}$.

## II. THE ELECTRONIC BAND STRUCTURE OF NAALSI WITHOUT SOC ALONG THE NON-HIGH SYMMETRY LINE

From Fig.S2(b), we can see that there are also have band crossing around Γ and Z points along the non-high symmetry line. It confirms that the energy band crossing ($C_{1-8}$) around Γ and Z points mentioned before are not isolated points.

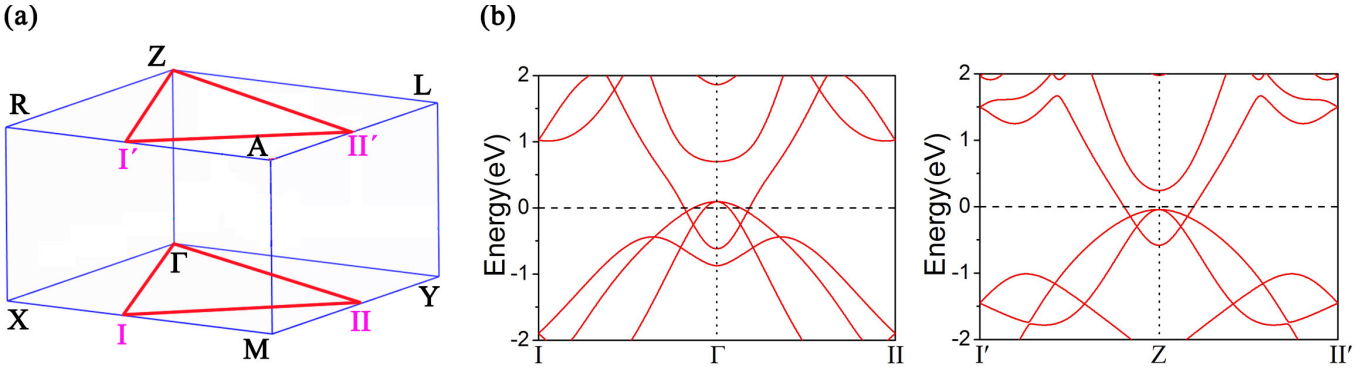


Figure S2: (color online) (a) The path along non-high symmetry line in BZ. (b) The electronic band structure along the non-high symmetry line.

## III. THE ELECTRONIC BAND STRUCTURE OF NAALSI WITHOUT SOC AND WITH SOC.

Compare with the fig.2(a), we plot an enlarged view of the nodal line around Z point in fig.S3(a). The crossing points label as $C_5$, $C_6$, $C_7$ and $C_8$ near Z point. The crossing points of $C_5$ and $C_6$ (belong to hybrid nodal line) contribute by Al-s and Si-$p_y$ orbital, and the points of $C_7$ derives from Al-s and Si-$p_x$ and $C_8$ from Al-s and Si-$p_y$ orbital which same as the crossing point around Γ point. The band structure of NaAlSi with SOC is shown in fig.S3(b). All crossing points open a band gap less than 10meV can be seen clearly in the enlarged picture of Fig.S2(c-d).

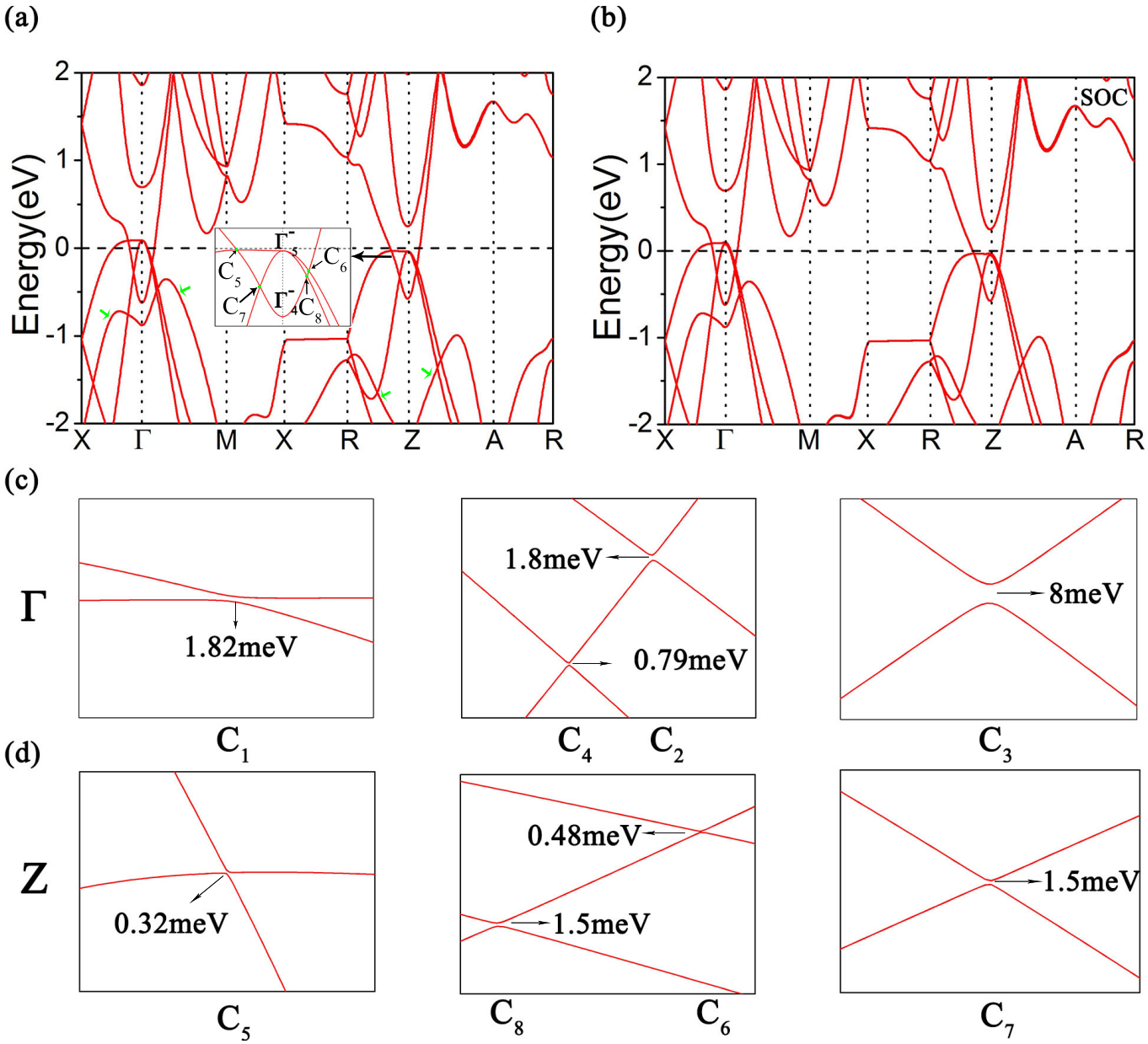


Figure S3: (color online) (a) The electronic band structure of NaAlSi (The insertion graph is an enlarged view of the nodal line near the point of Z). (b) The electronic band structure of NaAlSi with SOC. (c-d) The enlarged view of the electronic band structure with SOC for $C_{1-8}$ points.

## IV. THE TOPOLOGICAL SURFACE STATES OF NAALGE.

We plot the local density of states for NaAlGe with semi-infinite edge in the fig.S4. In our surface states computation, we chosen paths $\overline{X}$-$\overline{\Gamma}$-$\overline{Z}$-$\overline{X}$ along the high symmetry line to show the edge state of the nodal line between the Γ and Z point in BZ. Another we selection the path of $\overline{X}$-$\overline{\Gamma}$-$\overline{X}$ to shown the surface state of the nodal line around the Γ point. Topological nontrivial surface states are found in both two graph in fig.S4(a)-(b).

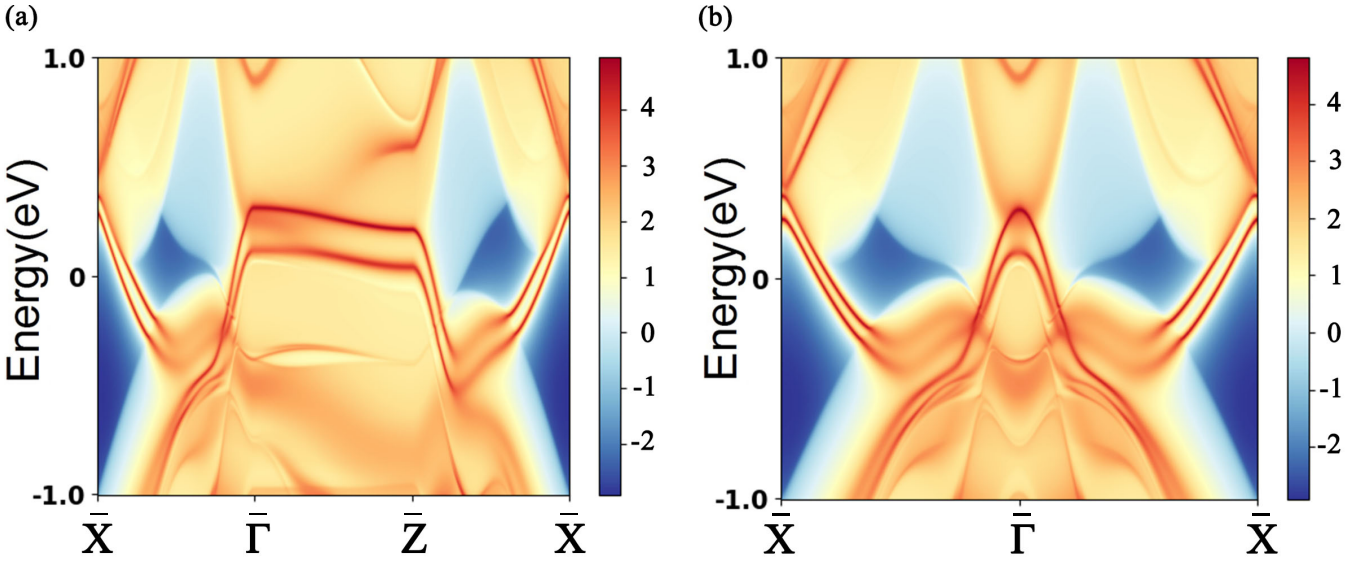


Figure S4: (color online) (a)-(d)The local density of states for NaAlSi with different paths $\overline{X}$-$\overline{\Gamma}$-$\overline{Z}$-$\overline{X}$ and $\overline{X}$-$\overline{\Gamma}$-$\overline{X}$.

## V. THE ELECTRONIC BAND STRUCTURE OF NAALGE WITHOUT SOC AND WITH SOC.

We have also calculated the band structure of NaAlGe both without SOC and with SOC are shown in fig.S5. From the figure we can see that NaAlGe have similar band structure with NaAlSi when SOC is not considered. Differen from NaAlSi, when SOC is considered, NaAlGe opens up a larger bandgap which can be clearly seen in the fig.S5(b). The band gaps in $k_z$=0 plane are 46.7meV, 2.39meV, 43.3meV, and 5.4meV for $C_1$, $C_2$, $C_3$, and $C_4$, respectively. The band gaps in $k_z$=$\pi$/a plane are 1.64meV, 3.81meV, 3.74meV, and 3.91meV for $C_5$, $C_6$, $C_7$, and $C_8$, respectively.

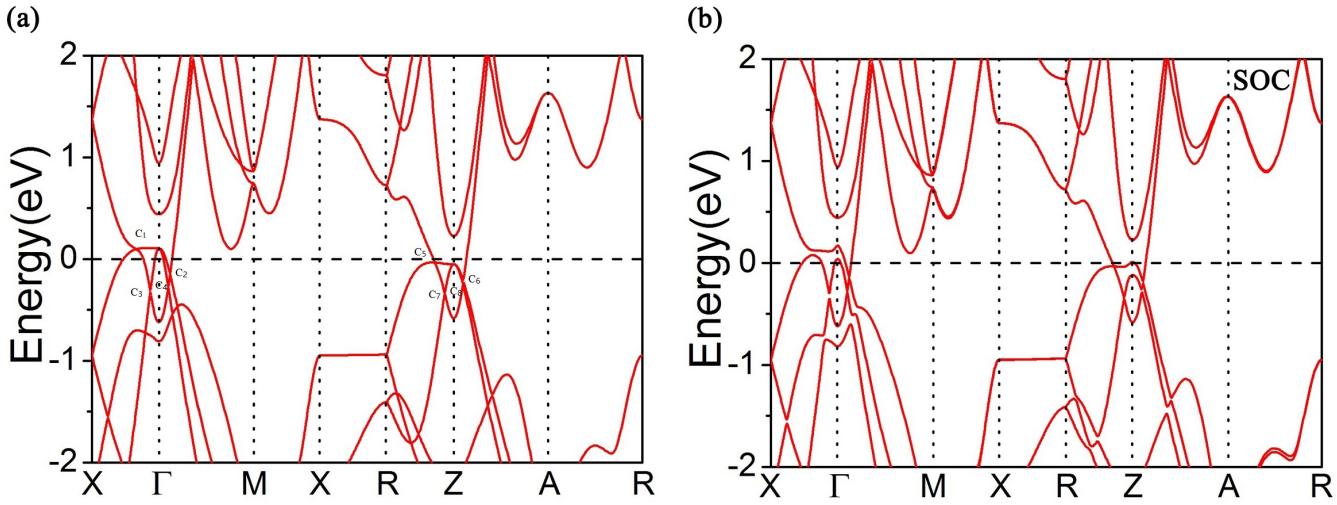


Figure S5: (color online) (a)-(d)The electronic band structure of NaAlGe without SOC and with SOC.

## VI. 3D BAND STRUCTURE OF NAALSI BASED ON *K·P* MODEL

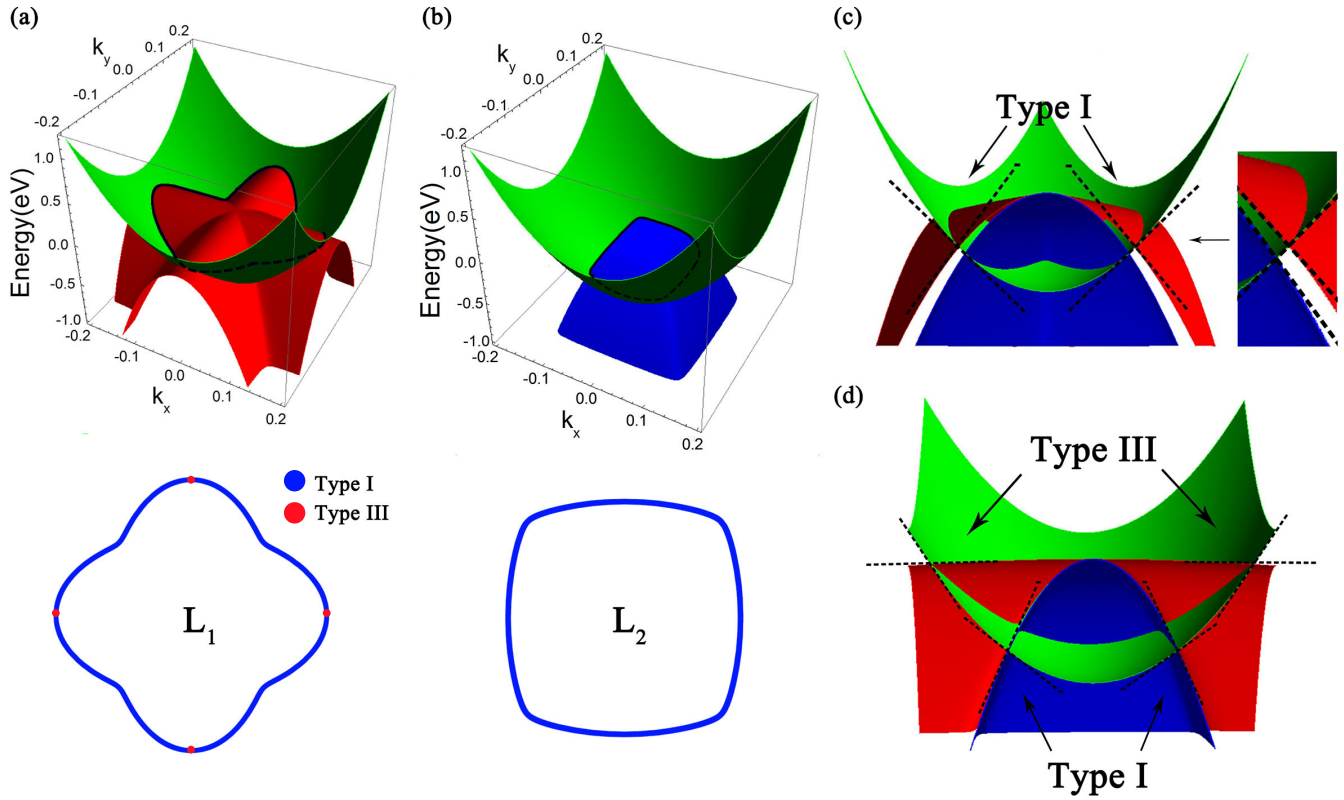


Figure S6: (color online) Up-panels of (a) and (b) are 3D band structures of ① +② and ①+③ (as denoted in Fig.2 (a)) around Γ point. The down-panels of (a) and (b) are the nodal lines between ① +② and ①+③, respectively. The red dots are the type-III nodal points. (c) and (d) are section view of the 3D band structures of ① +②+③ along (110) and (100) directions in the $k_z = 0$ plane, respectively.

## VII. MIGRATION PATHS AND DIFFUSION ENERGY OF NA FOR NAALGE.

The schematic representation of the Na migration and energy profiles pathways for NaAlGe are plotted in Fig.S7. We investigated the possible migration pathways which named as path 1 and path 2. From the energy profiles in Fig.S7(b), the energy barrier is estimated to be 0.358eV and 0.79eV for Na atoms diffuse along path 1 and path 2, respectively. The average voltage of NaAlGe with different concentration of Na is also presented in Fig.S7(c). We found it share the similar character of NaAlSi of main manuscript.

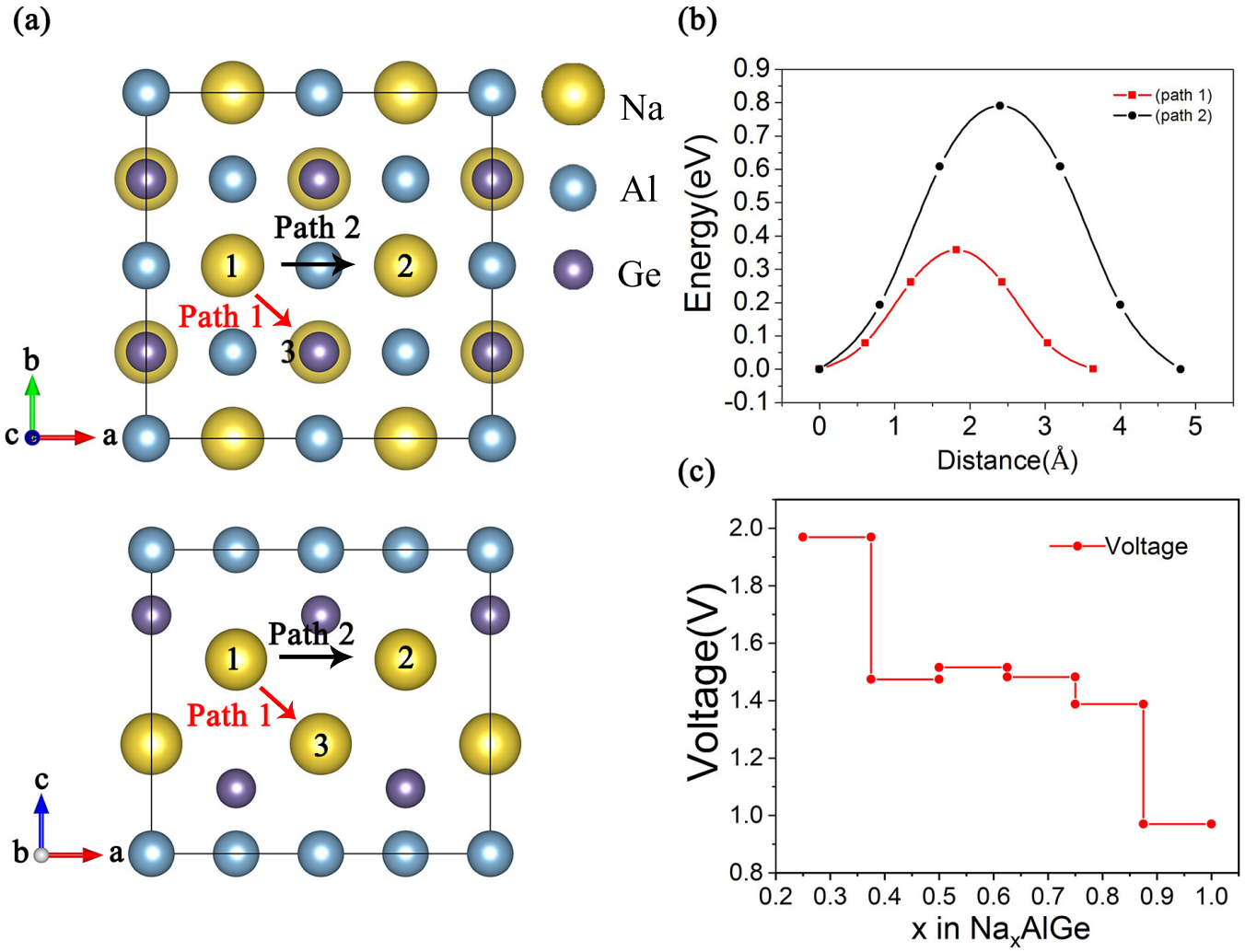


Figure S7: (color online)(a) Two possible migration paths for Na diffusion of NaAlGe. (b) Diffusion energy of Na for NaAlGe. (c) The average voltage profile for $Na_xAlGe$(x = 0.125, 0.25, 0.375, 0.5, 0.625, 0.75) with different concentration of Na.

## VIII. DENSITY OF STATES OF $NA_xALSI$ WITH 2 × 2 × 1 SUPERCELL

Here we use the density of states(DOS) around Fermi level characterize the electronic conductivity with different concentrations of Na with 2 × 2 × 1 supercell(NaxAlSi, x = 0.125, 0.25, 0.375, 0.5, 0.625, 0.75 ). The results are shown in following Fig.S8. We found the NaAlSi always keep metallic feature under different concentrations of Na. Moreover, in x = 0.125, 0.375, 0.625, 0.75, the values of DOS are relatively higher than other concentration of Na.

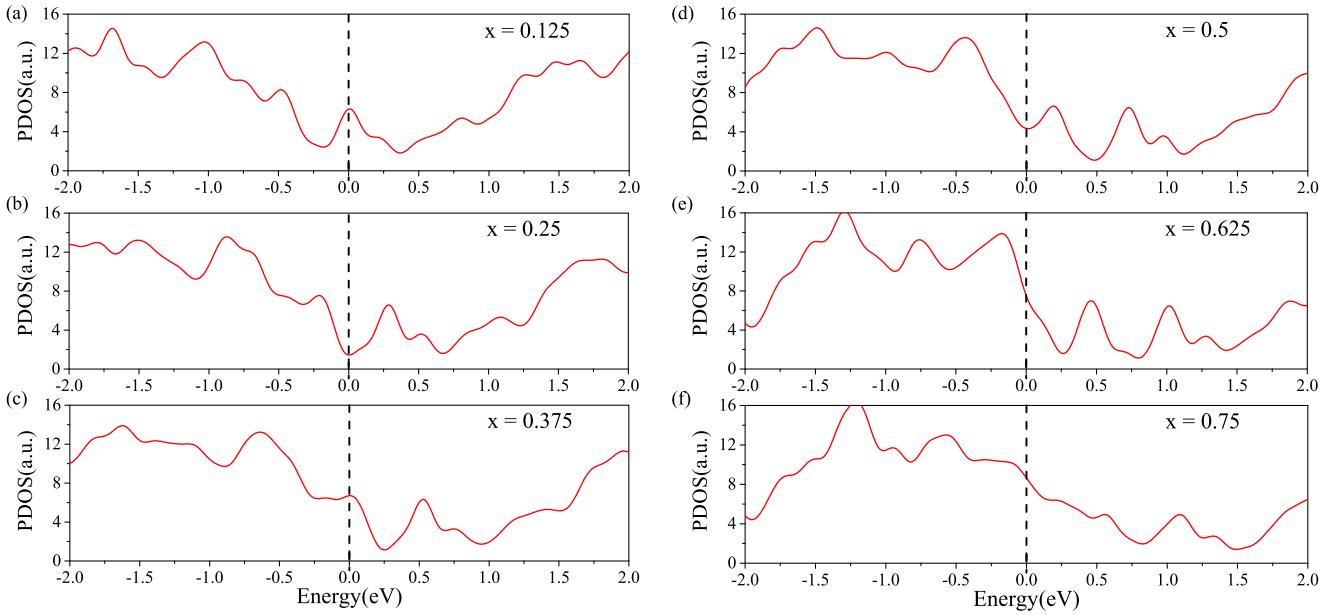


Figure S8: (color online) Density of states of $Na_xAlSi$ with (a) x = 0.125 (b) x = 0.25 (c) x = 0.375 (d) x = 0.5 (e) x = 0.625 (f) x = 0.75.

* Electronic address: zhoupan71234@xtu.edu.cn
† Electronic address: lzsun@xtu.edu.cn